Spectroscopic Properties of Binuclear Palladium(0) and Platinum(0) Dibenzylideneacetone Complexes

Pierre D. Harvey,[1a] Fran Adar,[1b] and Harry B. Gray*,[1a]

Contribution No. 7686 from the Arthur Amos Noyes Laboratory, California Institute of Technology, Pasadena, California 91125, and Instruments SA, Edison, New Jersey 08820. Received June 6, 1988

Abstract: The UV–visible absorption, excitation, and emission spectra of $M_2(dba)_3$ in 2-MeTHF at 295 and 77 K, and the resonance Raman spectra of solid $M_2(dba)_3$ and dba (M = Pd, Pt; dba = dibenzylideneacetone) at 295 K, have been investigated. The MLCT (18 600 cm^{-1}, Pd; 17 300 cm^{-1}, Pt) and $p\sigma \leftarrow d\sigma^*$ (26 300 cm^{-1}, Pd; 25 300 cm^{-1}, Pt) transitions are assigned on the basis of solvent polarity and metal dependences of the absorption maxima and by comparison with $M_2(dppm)_3$ (M = Pd, Pt; dppm = bis(diphenylphosphino)methane) spectral data. The $\nu(M-M)$ values ($\nu(Pd-Pd) = 76$ cm^{-1}, $F = 0.18$ mdyn Å^{-1}; $\nu(Pt-Pt) = 72$ cm^{-1}, $F = 0.30$ mdyn Å^{-1}) indicate that the M–M interactions are relatively weak. Based on absorption–emission energy gaps and on the relatively long emission lifetimes, the emission bands (13 500 cm^{-1}, Pd; 12 500 cm^{-1}, Pt) are assigned to MLCT triplet → singlet transitions.

Investigations of d^8–d^8 M_2 (M = Rh, Ir, Pt) complexes have shown that the lowest electronic excited states are derived from $p\sigma \leftarrow d\sigma^*$ transitions and that the M–M bonding in these states is enhanced over that observed in the ground state.[2-7] The spectroscopic and photophysical properties of d^{10}–d^{10} dipalladium and diplatinum phosphine complexes also have been reported;[8,9] an absorption band attributable to the $p\sigma \leftarrow d\sigma^*$ transition appears in the visible region, thereby indicating the presence of M–M interactions in these species.

We have extended our work on d^{10}–d^{10} systems to include $M_2(dba)_3$ (M = Pd, Pt; dba = dibenzylideneacetone) complexes.[10-12] Of special interest here are the ground-state M–M interactions and the assignments of the lowest electronic excited states.

Experimental Section

Materials. 4,4′-Dimethoxydibenzylideneacetone (dba-OMe),[10] dba,[10] $M_2(dba)_3$ (M = Pd,[11] Pt[12]), and $Pd_2(dba-OMe)_3$[11] were synthesized according to standard procedures. The complexes were purified by triple recrystallization in benzene/ethyl ether. Purity was checked by elemental analysis and ^{1}H NMR spectroscopy (500 MHz; 1000 scans). 2-MeTHF (Aldrich) was purified according to a standard procedure.[13] Benzene and chloroform (B&J) were used without further purification. All spectroscopic measurements were made after freeze–pump–thaw degassing of the solutions.

Measurements. The UV–visible absorption spectra were measured on Cary 17 (77 K) and Hewlett Packard 8450A diode array (room-temperature) spectrophotometers. The emission and excitation spectra were obtained with a Perkin-Elmer MPF-66 spectrofluorometer. The emission lifetimes were measured on a Quanta Ray Nd-YAG (8-ns fwhm; 532-nm excitation) laser system.[14] The solid-state resonance Raman (RR) spectra were recorded on an ISA microRaman Jobin Yvon U-1000 spectrometer, by using the 454.5-, 488.0-, 514.5-, and 568.2-nm lines of argon and krypton ion lasers.

Results and Discussion

The first syntheses of $M_2(dba)_3 \cdot$solvent (solvent = CHCl$_3$, CH$_2$Cl$_2$, C$_6$H$_6$, and dba) were published in the early 1970s.[11,12] These complexes are remarkably air-stable both in the solid state and in solutions, and their molecular structures have been investigated by X-ray crystallography[15,16] and ^{1}H NMR spectroscopy.[17,18] The structure determinations have shown[15-18] that the geometry is the same in the solid state and in solution. Electrochemical investigations show that the complexes exhibit a series of relatively reversible one-electron reductions centered on the dba ligands and one irreversible one-electron metal oxidation.[19-21]

Electronic Absorption Spectra. The UV–visible spectra of dba and $M_2(dba)_3$ in 2-MeTHF at 295 and 77 K are shown in Figures 1 and 2. The $Pd_2(dba)_3$ spectra exhibit three intense absorption bands in the 300–600-nm region: a broad band at ~520 nm, a shoulder at 380 nm, and a strong, vibrationally structured band at ~350 nm (77 K). Assignment of the 350-nm band to a ligand-localized transition is indicated by a comparison of the 77 K spectra of $Pd_2(dba-OMe)_3$ and dba-OMe; band shapes and

(1) (a) California Institute of Technology. (b) Instruments SA.
(2) Roundhill, D. M.; Gray, H. B.; Che, C.-M. *Acc. Chem. Res.*, in press.
(3) (a) Marshall, J. L.; Stiegman, A. E.; Gray, H. B. ACS Symposium Series 307, Lever, A. B. P., Ed.; American Chemical Society: Washington, DC, 1986; p 166. (b) Che, C.-M.; Lee, W. M. *J. Chem. Soc., Chem. Commun.* **1986**, 512. (c) Roundhill, D. M. *J. Am. Chem. Soc.* **1985**, *107*, 4354. (d) Peterson, J. R.; Kalyanasundaram, K. *J. Phys. Chem.* **1985**, *89*, 2486. (e) Che, C.-M.; Butler, L. G.; Grunthaner, P.; Gray, H. B. *Inorg. Chem.* **1985**, *24*, 4662. (f) Kim, J.; Fan, F. F.; Bard, A. J.; Che, C.-M.; Gray, H. B. *Chem. Phys. Lett.* **1985**, *121*, 543. (g) Che, C.-M.; Butler, L. G.; Gray, H. B. *J. Am. Chem. Soc.* **1981**, *103*, 7796. (h) Fordyce, W. A.; Crosby, G. A. *J. Am. Chem. Soc.* **1982**, *103*, 7061.
(4) (a) Rice, S. F.; Milder, S. J.; Gray, H. B.; Goldbeck, R. A.; Kliger, D. S. *Coord. Chem. Rev.* **1982**, *43*, 349, and references therein. (b) Gray, H. B.; Maverick, A. W. *Science* **1981**, *214*, 1201. (c) Eidem, P. K.; Maverick, A. W.; Gray, H. B. *Inorg. Chem.* **1981**, *50*, 50. (d) Mann, K. R. DiPierro, M. J.; Gill, T. P. *J. Am. Chem. Soc.* **1981**, *102*, 3965.
(5) (a) Marshall, J. L.; Stobart, S. R.; Gray, H. B. *J. Am. Chem. Soc.* **1984**, *106*, 3027. (b) Winkler, J. R.; Marshall, J. L.; Netzel, T. L.; Gray, H. B. *J. Am. Chem. Soc.* **1986**, *108*, 2263.
(6) (a) Che, C.-M.; Butler, L. G.; Gray, H. B.; Crooks, R. M.; Woodruff, W. H. *J. Am. Chem. Soc.* **1983**, *105*, 5492. (b) Rice, S. F.; Gray, H. B. *J. Am. Chem. Soc.* **1981**, *103*, 1593. (c) Dallinger, R. F.; Miskowski, V. M.; Gray, H. B.; Woodruff, W. H. *J. Am. Chem. Soc.* **1981**, *103*, 1595.
(7) Zipp, A. P. *Coord. Chem. Rev.* **1988**, *84*, 47.
(8) Caspar, J. V. *J. Am. Chem. Soc.* **1985**, *107*, 6718.
(9) Harvey, P. D.; Gray, H. B. *J. Am. Chem. Soc.* **1988**, *110*, 2145.
(10) Conrad, C. R.; Dolliver, M. A. *Organic Syntheses*; Wiley: New York, 1943; Collect. Vol. 11, p 167.
(11) Takahashi, Y.; Ito, T.; Ishii, Y. *J. Chem. Soc., Chem. Commun.* **1970**, 1065.
(12) Moseley, K.; Maitlis, P. M. *J. Chem. Soc., Chem. Commun.* **1971**, 982.
(13) 2-Methyltetrahydrofuran was purified according to the procedure outlined for tetrahydrofuran in: Gordon, A. J.; Ford, R. A. *The Chemist's Companion, A Handbook of Practical Data, Techniques, and References*; Wiley: New York, 1972; p 436.
(14) Nocera, D. G.; Winkler, J. R.; Yocom, K. M.; Bordignon, E.; Gray, H. B. *J. Am. Chem. Soc.* **1984**, *106*, 5145.
(15) (a) Mazza, M. C.; Pierpont, C. G. *J. Chem. Soc., Chem. Commun.* **1973**, 207. (b) Pierpont, C. G.; Mazza, M. C. *Inorg. Chem.* **1974**, *13*, 1891.
(16) Ukai, T.; Kawazura, H.; Ishii, Y.; Bonnet, J.-J.; Ibers, J. A. *J. Organomet. Chem.* **1974**, *65*, 253.
(17) Kawazura, H.; Tanaka, H.; Yamada, K.; Takahashi, T.; Ishii, Y. *Bull. Chem. Soc. Jpn.* **1978**, *51*, 3466.
(18) Tanaka, H.; Ishii, H.; Kawazura, H. *Bull. Chem. Soc. Jpn.* **1979**, *52*, 2815.
(19) Ito, N.; Aoyagui, S.; Saji, T. *J. Electroanal. Chem. Interfacial Chem.* **1981**, *130*, 357.
(20) Ito, N.; Saji, T.; Aoyagui, S. *J. Electroanal. Chem. Interfacial Chem.* **1983**, *144*, 153.
(21) Harvey, P. D.; Thorp, H. H.; Gray, H. B., unpublished results.

Table I. Spectroscopic Data for d^{10}–d^{10} Pd_2 and Pt_2 Complexes[a]

	pσ ← dσ*	MLCT	emission	λ(pσ → dσ*) − $λ_{em}$	λ(MLCT) − $λ_{em}$
$Pd_2(dba)_3$[b]	26 300 (38 400)	18 600 (19 500)	13 500	12 800	5100
$Pt_2(dba)_3$[b]	25 300 (34 000)	17 300 (65 000)	12 500	12 800	4800
$Pd_2(dppm)_3$[c]	22 700 (33 800)		14 400	8 300	
$Pt_2(dppm)_3$[c]	20 800 (27 400)		12 700	8 100	

[a] 2-MeTHF solutions at 77 K [cm^{-1} (ϵ in M^{-1} cm^{-1})]. [b] This work. [c] Data from ref 9.
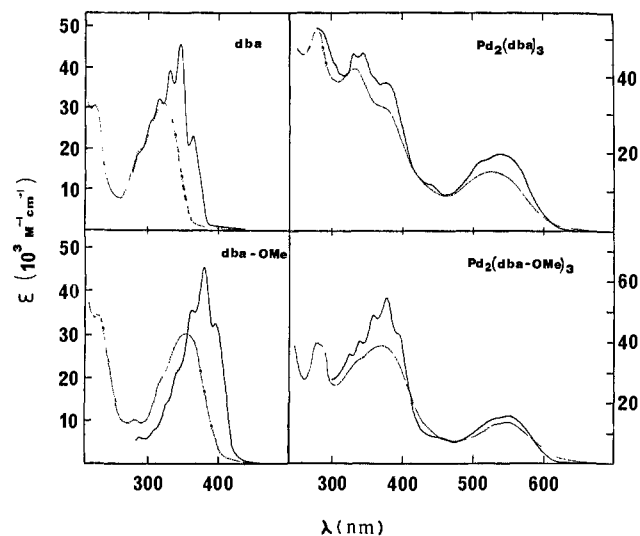
Figure 1. UV–visible absorption spectra of dba, $Pd_2(dba)_3$, dba-OMe, and $Pd_2(dba-OMe)_3$ in 2-MeTHF solution at 295 (···) and 77 K (—).
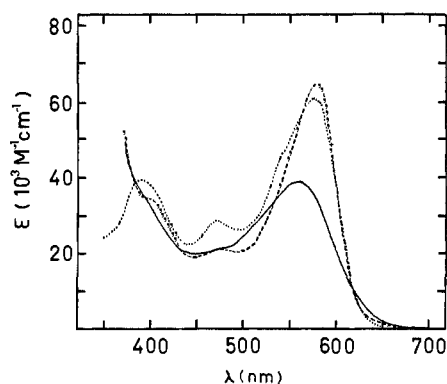

Figure 2. UV–visible absorption (295 (—), and 77 K (- - -)) and excitation (77 K (···)) spectra of $Pt_2(dba)_3$ in 2-MeTHF.

Figure 3. UV–visible absorption spectra of $M_2(dba)_3$ in C_6H_6 (1), THF (2), and $CHCl_3$ (3) at 295 K. Intensities of the 520- and 560-nm bands have been normalized.

Figure 4. RR spectra of solid $M_2(dba)_3$ at room temperature in the 30–600-cm^{-1} (M = Pd) and 50–300-cm^{-1} (M = Pt) regions. Experimental conditions. M = Pd: laser excitation, 514.5 nm; laser power, 1 mW at the sample; slits, 300 μm; 1s/data point, 5 scans. M = Pt: same as for Pd, except slits at 400 μm and 4 scans.

positions of the vibrational progressions correspond closely in these cases. The bands at ~520 and ~560 nm in the spectra of $Pd_2(dba)_3$ and $Pt_2(dba)_3$, respectively, are assigned to MLCT. An MLCT assignment is supported by the solvent and M dependences of $λ_{max}$ (Figure 3; $λ_{max}$ = 520, 522, and 530 nm for M = Pd; $λ_{max}$ = 560, 564, and 570 nm for M = Pt in C_6H_6, 2-MeTHF, and $CHCl_3$).

The 380- and 400-nm shoulders in the spectra of $Pd_2(dba)_3$ and $Pt_2(dba)_3$, respectively, which are solvent independent (±2 nm), become significantly more resolved at 77 K (ϵ = 38 400 M^{-1} cm^{-1}, M = Pd; 34 000 M^{-1} cm^{-1}, M = Pt). It is likely that these features are related to the intense (ϵ ~ 30 000 M^{-1} cm^{-1} at 77 K) pσ ← dσ* bands in $M_2(dppm)_3$ complexes, which occur at 440 nm (Pd) and 480 nm (Pt).[9] Since Pd–Pd is longer for $Pd_2(dba)_3$ (r(Pd–Pd) = 3.24 Å)[15,16] than for $Pd_2(dppm)_3$ (r(Pd–Pd) = 3.043 Å; RR measurements),[9] the pσ ← dσ* transition should be significantly blue-shifted for $Pd_2(dba)_3$; $λ_{max}$ < 440 nm. Assuming that r-(Pt–Pt) is not very different from r(Pd–Pd), a similar situation should obtain for $Pt_2(dba)_3$. Thus, the 380-nm (Pd) and 400-nm (Pt) shoulders are assigned to ^{1}(pσ ← dσ*). Spectroscopic data for the Pd_2 and Pt_2 complexes are given in Table I.

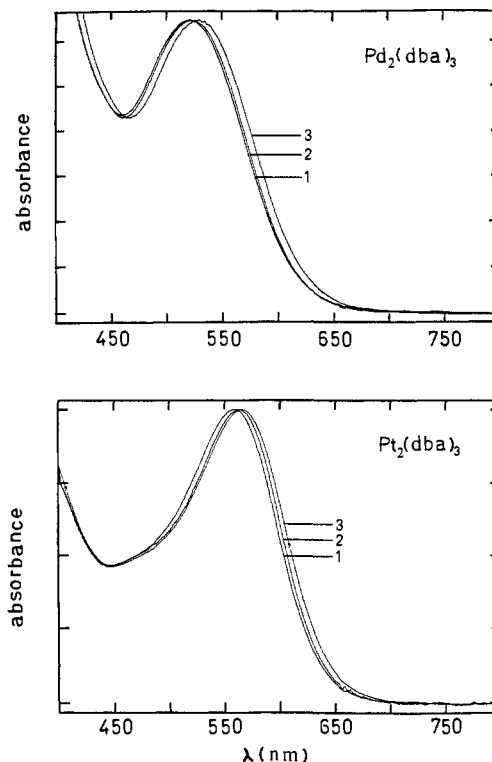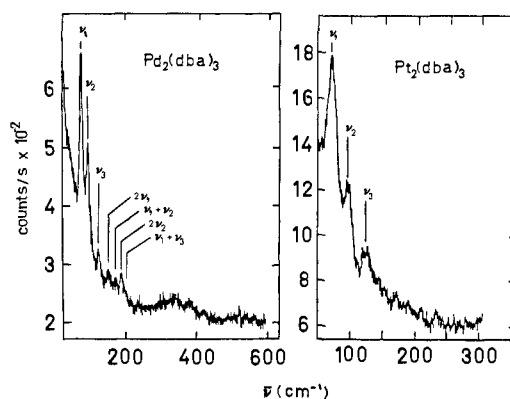**Resonance Raman Spectra.** The RR spectra[22] of solid $M_2(dba)_3$

complexes in the 10–300-cm^{-1} region at room temperature are shown in Figure 4. The Raman spectrum of solid dba is fea-

(22) Measurements of the Raman spectra using different $λ_{exc}$, 454.5, 488.0, 514.5, and 564.2 nm, have shown that the Raman intensities are significantly $λ_{exc}$ dependent. The intensity reaches a minimum value at 564.2 nm (20 counts) and optimum signal at 488.0 nm (~500 counts) (averaged at 5 scans, 1-mW laser power at the sample, and 300-μm slit aperture). Due to the lack of Raman data with $λ_{exc}$ < 454.5 nm, a complete profile was not obtained. The sensitivity of the Raman intensity to $λ_{exc}$ confirms the resonance of the vibrational modes.

Table II. Ground-State Spectroscopic and Structural Parameters for Pd$_2$ and Pt$_2$ Complexes

	ν(M–M), cm^{-1}	F(M–M),[b] mdyn Å^{-1}	r(M–M) calc[c]	r(M–M) X-ray
Pd$_2$(dba)$_3$[a]	76	0.18	3.18	3.241[d]
Pt$_2$(dba)$_3$[a]	72	0.30	3.16	
Pd$_2$(dppm)$_3$[e]	120	0.45	3.04	
Pt$_2$(dppm)$_3$[e]	102.5	0.60	3.02	3.024[f]
Pt$_2$(pcp)$_4^{4-}$	113[g]	0.73	2.97	2.980[g]
Pt$_2$(pop)$_4^{4-}$	118[h]	0.80	2.94	2.925[i]

[a] This work. [b] $F = \mu(2\pi\nu)^2$. [c] Equations 1 and 2. [d] Average value taken from ref 15 and 16. [e] From ref 9. [f] From: Manojlovic-Muir, L. J.; Muir, K. W. *J. Chem. Soc., Chem. Commun.* **1982**, 1155. Manojilovic-Muir, L.; Muir, K. W.; Grossel, M. C.; Brown, M. P.; Nelson, C. D.; Yavari, A.; Kallas, E.; Moulding, R. P.; Seddon, K. R. *J. Chem. Soc., Dalton Trans.* **1980**, 1955. [g] From: King, C.; Auerbach, R. A.; Fronczek, F. R.; Roundhill, D. M. *J. Am. Chem. Soc.* **1986**, *108*, 5626. [h] From ref 6a. [i] From: Filomena dos Remedios Pinto, M. A.; Sadler, P. J.; Neidle, S.; Sanderson, M. R.; Kuroda, R. *J. Chem. Soc., Chem. Commun.* **1980**, *13*. Marsh, R. E.; Herbstein, F. H. *Acta Crystallogr.* **1983**, *B39*, 280.

tureless in this region. Peaks attributable to ν(M–M), ν_1, are at 76 cm^{-1} (M = Pd) and 72 cm^{-1} (M = Pt). Woodruff's equations relating bond distances (r in angstroms) and force constants (F in millidynes per angstrom) for M$_2$ complexes of the 4d and 5d series are[23]

$$r(4d) = 1.83 + 1.45 \exp(-F/2.53) \qquad (1)$$

$$r(5d) = 2.01 + 1.31 \exp(-F/2.36) \qquad (2)$$

Values of 3.18 and 3.16 Å are obtained for Pd and Pt, respectively. The ν_1 value remains the same upon substitution in the para position of the dba phenyl ring. The Raman peaks at $\sim$95 cm^{-1} (ν_2) and 126 cm^{-1} (ν_3) are assigned to $\|$–M–$\|$ bending modes, while the weaker features (152 cm^{-1} (2ν_1), 170 cm^{-1} ($\nu_1 + \nu_2$), 188 cm^{-1} (2ν_2), and 202 cm^{-1} ($\nu_1 + \nu_3$)) are assigned to overtones and combinations. Observation of overtones and combinations of ν(M–M) in the RR spectra of M$_2$ complexes is a strong indication of M–M-localized transitions.[24]

Surprisingly, no Raman band associated with the dba ligand is observed in the 400–1800-cm^{-1} region for the M$_2$ compounds, even using λ_{exc} = 514.5 and 564.2 nm with a very large number of scans; ν_2 and ν_3 should also be RR-enhanced upon MLCT excitation, but the ratios $I(\nu_1)/I(\nu_2)$ and $I(\nu_1)/I(\nu_3)$ did not vary with λ_{exc}. The presence of ν(M–M) in the M$_2$ complexes clearly indicates that M–M-localized transitions occur in the electronic spectra. The intensity dependence of ν(M–M) with λ_{exc} confirms that those transitions should be at λ < 488.0 nm.

Table II compares the ground-state vibrational and structural parameters for several Pd$_2$ and Pt$_2$ species. The M$_2$(dba)$_3$ complexes exhibit the smallest F's and longest r(M–M)'s, indicating that the M–M interactions are relatively weak. The X-ray crystal structure of Pt$_2$(dba)$_3$ has not been reported. Since r(M–M) shrinks by 0.02 Å going from Pd$_2$(dppm)$_3$ to Pt$_2$(dppm)$_3$, a similar effect is assumed for the M$_2$(dba)$_3$ complexes, and d(Pt–Pt) is estimated to be 3.22 Å for Pt$_2$(dba)$_3$.

Polarized Spectra. Crystals of suitable size for single-crystal polarized spectroscopy have not been obtained. Fortunately, because the M$_2$(dba)$_3$ complexes exhibit strong emission in a 2-MeTHF glass at 77 K, the photoselection technique can be used.[25] To obtain absorption polarizations by this method, we must know the emission polarization relative to the molecular axis. For the M$_2$(dba)$_3$ complexes, these relatively long-lived emissions arise from an MLCT state; they will be discussed in more detail in the following section. The lowest allowed electronic transitions are polarized in the xy plane; ML$_3$ defines the plane,[26] and these
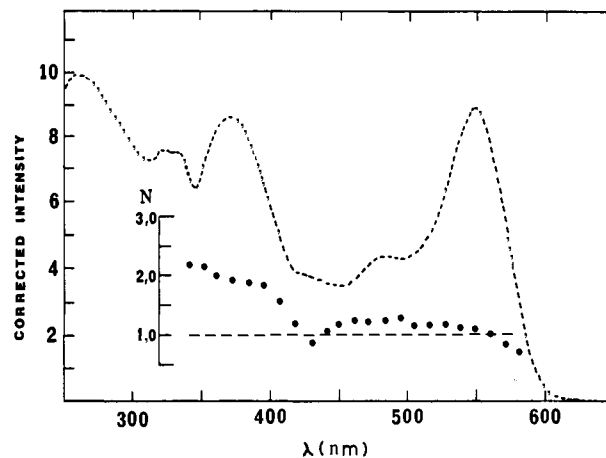
Figure 5. Excitation spectrum and the emission excitation polarization ratios for Pd$_2$(dba)$_3$ in 2-MeTHF at 77 K.
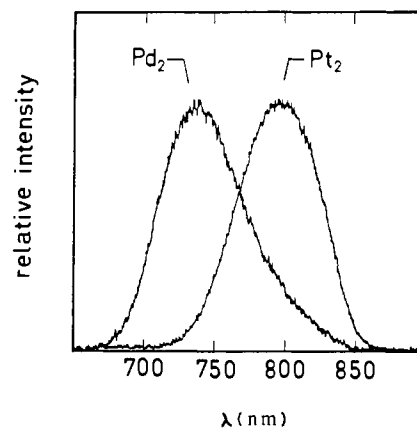
Figure 6. Emission spectra of M$_2$(dba)$_3$ in 2-MeTHF at 77 K.

emissions are $\perp$-polarized. However, a large degree of depolarization of the MLCT band is expected, as X-ray crystallographic studies indicate that the olefins are not aligned rigorously (parallel) with the xy plane.[15,16] The excitation spectrum and polarization ratios for Pd$_2$(dba)$_3$ are shown in Figure 5. The polarization ratio, N, is given by $(I_{BB}/I_{BE})_V(I_{EE}/I_{EB})_H$, where $(I_{BB}/I_{BE})_V$ is the ratio of the intensities of vertically to horizontally polarized emission when excited with vertically polarized light and $(I_{EE}/I_{EB})_H$ is the ratio of the intensities of $\|$- and $\perp$-polarized emission with horizontally polarized excitation. N is then related to the relative orientation of transition moments in absorption and emission. The theoretical value of N = 3 indicates absorption polarized along a single molecular axis followed by emission along the same axis. N = 0.5 indicates single-axis absorption followed by emission along a perpendicular axis. (In practice, the theoretical values were never obtained; this is due in part to the natural depolarization of the glass.) $N \sim$ 1.2 from 430 to 580 nm (throughout the MLCT band) indicates a large degree of depolarization. In the 350–400-nm range, $N \sim$ 2 shows that a significant component of the 380-nm band is polarized parallel to the emission. It follows that the singlet p$\sigma \leftarrow$ dσ^* transition most likely is associated with the 380-nm absorption. A polarization measurement was not attempted in the case of Pt$_2$(dba)$_3$.

Emission Spectra and Lifetimes. Emission spectra of M$_2$(dba)$_3$ are shown in Figure 6. Because r(M–M)(M$_2$(dba)$_3$) > r(M–M)(M$_2$(dppm)$_3$), the emission maximum should blue-shift from M$_2$(dppm)$_3$ to M$_2$(dba)$_3$, if the nature of the emissive state is the

(23) (a) Woodruff, W. H., unpublished results. (b) Miskowski, V. M.; Dallinger, R. F.; Christoph, G. G.; Morris, D. E.; Spies, G. H.; Woodruff, W. H. *Inorg. Chem.* **1987**, *26*, 2127.
(24) Clark, R. J. H.; Stewart, B. *Struct. Bonding (Berlin)* **1978**, *36*, 1.
(25) (a) Harvey, P. D.; Durocher, G. *Spectrosc. Int. J.* **1983**, *2*, 128. (b) Parker, W. L.; Crosby, G. A. *Chem. Phys. Lett.* **1984**, *105*, 544.

(26) The lowest allowed MLCT transitions for complexes of the type [M(C=C)$_3$]$_2$ (D_{3h} symmetry), where all olefins lie out of the ML$_3$ plane, are polarized along this plane. By perpendicularly rotating one of the three olefins, the local symmetry is reduced to C_{2v} and the lowest energy transition is also polarized in this plane. However, $\perp$-polarized allowed transitions lie nearby. Further reduction of the local symmetry around M contributes to the depolarization of the MLCT.

Table III. Emission Lifetimes at λ_{max} for Pd$_2$ and Pt$_2$ Complexes

	τ_e, μs (λ_{max}, nm)	
	295 K	77 K
Pd$_2$(dba)$_3$[a]	0.22 ± 0.01 (740)	8.0 ± 0.2 (740)
Pt$_2$(dba)$_3$[a]	0.23 ± 0.01 (800)	0.95 ± 0.2 (800)
Pd$_2$(dppm)$_3$[b]	5.93 ± 0.01 (710)	107 ± 1 (685)
Pt$_2$(dppm)$_3$[b]	<0.02 (790)	10.6 ± 0.2 (790)
Pt$_2$(pop)$_4$[4-]	9.8 (517[c])	10.3 (515[d])
Pt$_2$(pcp)$_4$[4-][e]	0.055 (510)	10.0 (510)

[a] This work. [b] From ref 9. [c] From ref 3g. [d] From ref 3 h. [e] King, C.; Auerbach, R. A.; Fronczek, F. R.; Roundhill, D. M. *J. Am. Chem. Soc.* **1986**, *108*, 5626.

same. Exactly the opposite is observed. The energy gap between the singlet p$\sigma \leftarrow$ dσ^* and emission transitions is much too large in the M$_2$(dba)$_3$ cases ($\Delta \sim$ 12 800 cm^{-1}, which is $\sim$4600 cm^{-1} greater than Δ in the M$_2$(dppm)$_3$ complexes).[9] On the basis of transition energies, an M–M-localized emissive state is ruled out. Similarly, due to the M dependence of λ_{em}, the absence of a dba band in the excitation spectra (see Figures 2 and 5), and complete absence of dba luminescence in the 700–900-nm region, the possibility of emission arising from a ligand-localized state also is eliminated. The energy gap between the MLCT absorption and emission bands is $\sim$5000 cm^{-1} (for both complexes), which is

identical with the energy gap measured for Ru(bpy)$_3^{2+}$ (which also possesses a low-energy MLCT absorption system[27]). Considering the transition energies, it is likely that an MLCT triplet excited state is responsible for the emission in M$_2$(dba)$_3$.[28]

The emissions at 295 and 77 K are relatively long-lived and are comparable to τ_e of other Pd$_2$ and Pt$_2$ complexes (Table III). Interestingly, for the M$_2$(dba)$_3$ complexes, τ_e(Pd) = τ_e(Pt) at 295 K.[29] The significant decrease in τ_e from Pd$_2$(dppm)$_3$ to Pd$_2$(dba)$_3$ (5.93 to 0.22 μs at 295 and 107 to 8.0 μs at 77 K) indicates that the dba ligand possesses a high degree of flexibility.

(27) Hager, G. D.; Crosby, G. A. *J. Am. Chem. Soc.* **1975**, *97*, 7031.
(28) The same assignment has been suggested by Kane-Maguire and Wright: Kane-Maguire, N. A. P.; Wright, L. L.; Guckert, J. A.; Tweet, W. S. *Inorg. Chem.* **1988**, *27*, 2905.
(29) This equality in τ_e between Pd$_2$ and Pt$_2$ is coincidental. The ln (1/τ_e) vs 1/T lines have different slopes: Harvey, P. D.; Gray, H. B., unpublished results.

Free Energy Dependence of the Electronic Factor in Biological Long-Range Electron Transfer

Kurt V. Mikkelsen,[†] **Jens Ulstrup,**[*,‡] **and Merab G. Zakaraya**[‡,§]

Contribution from the Department of Chemistry, University of Aarhus, 8000 Aarhus C, Denmark, and Chemistry Department A, Building 207, The Technical University of Denmark, 2800 Lyngby, Denmark. Received July 5, 1988

Abstract: The donor and acceptor orbitals in long-range electron transfer are strongly exposed to environmental inertial polarization fluctuations. The most likely polarization at the moment of electron transfer is determined by the intersection region of two potential surfaces spanned by collective polarization coordinates and depends strongly on the temperature and reaction free energy. These effects must therefore be reflected in corresponding variation of the electronic transmission coefficient with these quantities and not solely in the nuclear Franck–Condon factors. We have estimated these effects for system parameters appropriate to intramolecular electron transfer in (NH$_3$)$_5$Ru^{3+}- and Zn^{2+}-modified myoglobin. The estimates rest on variational calculation of a set of exponential trial wave functions in the instantaneous inertial polarization field and on a Hartree–Fock estimate of the distance decay of the Ru^{3+} and excited Zn orbitals involved. The effects are significant and dominated by a horizontal shift of the overall free energy relation by up to 0.5 eV toward numerically smaller values of the reaction free energy. This observation has important implications for electron tunnel distances in long-range electron transfer.

1. Introduction

Electron transfer between molecular centers separated by distances that notably exceed the geometric extension of the molecular reactant groups is of great importance in several contexts. "Long-range" electron transfer of this kind is, for example, a key element in multisite redox proteins,[1] in the electron-transfer sequences of photosynthesis and respiration,[2,3] and in intramolecular chemical[4–6] or biological[7–9] electron-transfer systems, where the donor and acceptor groups are separated by molecular bridge groups. Physically, rather similar features characterize crucial events in electrochemical electron transfer at surface-modified electrodes where the electron tunnels through a thin-surface oxide or polymer film and in inelastic tunneling assisted by local impurity or dislocation sites inside the surface film.[10–13]

Theoretical approaches specifically to long-range electron transfer have focused on the electronic factor in diabatic electron

[†] University of Aarhus.
[‡] The Technical University of Denmark.
[§] Permanent address: Institute of Inorganic Chemistry and Electrochemistry, Georgian Academy of Sciences, Tbilisi, USSR.

(1) (a) Peterson-Kennedy, S. E.; McGourty, J. L.; Kalweit, J. A.; Hoffman, B. M. *J. Am. Chem. Soc.* **1986**, *108*, 1739. (b) Kany, C. H.; Margoliash, E.; Ho, P.-S. *J. Am. Chem. Soc.* **1986**, *108*, 4665.
(2) DeVault, D. *Quantum Mechanical Tunnelling in Biological Systems*; Cambridge University Press: Cambridge, England, 1984.
(3) (a) *Antennas and Reaction Centres of Photosynthetic Bacteria*; Michel-Beyerle, M. E., Ed.; Springer-Verlag: Berlin, 1985. (b) *Structure of the Photosynthetic Bacterial Reaction Center: X-Ray Crystallography and Optical Spectroscopy with Polarized Light. NATO Advanced Workshop.* Breton, J., Vermeglio, A., Eds.; Plenum: New York, 1988.
(4) (a) Fischer, H.; Tom, G. M.; Taube, H. *J. Am. Chem. Soc.* **1976**, *98*, 5512. (b) Rieder, K.; Taube, H. *J. Am. Chem. Soc.* **1977**, *99*, 7891.
(5) Zawacky, S.; Taube, H. *J. Am. Chem. Soc.* **1981**, *103*, 3379.
(6) (a) Isied, S. S. *Prog. Inorg. Chem.* **1984**, *32*, 443. (b) Hush, N. S. *Coord. Chem. Rev.* **1985**, *64*, 135.
(7) (a) Kostič, N. M.; Margalit, R.; Che, C.-M.; Gray, H. B. *J. Am. Chem. Soc.* **1983**, *105*, 7765. (b) Margalit, R.; Kostič, N. M.; Che, C.-M.; Blair, D. F.; Chiang, H.-J.; Pecht, I.; Shelton, J. B.; Shelton, J. R.; Schroeder, W. A.; Gray, H. B. *Proc. Natl. Acad. Sci. U.S.A.* **1984**, *81*, 6554.